THE AMERICAN SOCIETY OF MECHANICAL ENGINEERS
345 E. 47th St., New York, N.Y. 10017

97-GT-202

INVESTIGATION OF TIP LEAKAGE EFFECTS IN TRANSONIC FLOW USING A PARALLEL UNSTRUCTURED NAVIER-STOKES CODE

C-W. Hustad and A. Bölcs
Swiss Federal Institute of Technology,
EPFL, 1015 - Lausanne, Switzerland.

M. Wehner
HBI Haerter AG,
8002 - Zurich, Switzerland.

ABSTRACT

Calculated results for tip flow around two different blade configurations are presented and compared with experimental data. The first configuration (case number 1) is a flat-plate profile tested in a linear transonic tunnel—the profile is an idealized representation of the aft-section of some highly curved turbine blades. The second configuration (case number 2) originates from the outer profile on the last-stage-blade of a steam turbine, however it is also reminiscient of a section from a turbine blade with supersonic exit flow. This configuration was tested in an annular cascade at Mach numbers representative of engine operating conditions.

The computed results were obtained using a parallel 3D unstructured Navier-Stokes code. The code runs on a workstation cluster, as well as being optimized for the 256 processor Cray T3D at EPFL: the code is capable of gigaflop performance using more than 3 million cells—adaptive mesh refinement thus allows enhanced resolution within the tip gap region.

For each configuration we have calculated two Runs. In both cases, Run-1 is similar to the experimental conditions, so that direct comparison between measured and calculated results is possible. With case number 1/Run-2 we re-calculated the flow without imposing a prescribed inflow boundary-layer along the sidewall. Comparison between the two runs helped reveal how free-stream total pressure can establish itself within the tip gap region. For the second configuration—in the annular cascade—we were interested in observing the influence of relative movement between the blade tip and adjacent sidewall. Hence for case number 2/Run-2 we imposed a circumferential velocity on the adjacent sidewall. This modified the effective sidewall boundary-layer and had a noticeable influence on the development of the tip-leakage flow.

NOMENCLATURE

M	= Mach number	h	= Enthalpy
X	= Chordwise coord.	p	= Pressure
Y	= Distance from sidewall	t	= Blade pitch
c	= Chord length	β	= Flow angle
d	= Profile thickness	β_g	= Stagger angle
		τ	= Tip gap height

ζ = Enthalpy loss coefficient, $(h_2-h_{2s})/(h_o-h_{2s})$

Subscripts

s	= Isentropic.		
o	= Stagnation.	1,2	= Inlet and Outlet.

INTRODUCTION

Tip leakage flow is an important phenomenum within turbomachinery and has, not surprisingly, received considerable attention, as witnessed by the available literature.

Early work by among others, Howell(1945), Ainley and Mathieson(1951), and Rains(1954), resulted in an empirical approach which formed the basis for development work during the following 20 years. It was only in the 1980's with the advent of new instrumentation techniques, together with improved CFD capabilities, that a clearer picture started emerging about the complexity of the flow within a gas turbine. This nurtured more detailed investigations into the source and mechanism by which losses arise. Such work is well described in the review by Denton(1993) who suggests that tip leakage losses may account for about one-third of the total loss. Interestingly he adds "...that an *a priori* prediction [of total loss] using the best available methods is unlikely to be accurate to better than ±20%". Needless to say, this not only underlines the complexity of the problem, but also the tremendous scope there is for improving our CFD capability.

Presented at the International Gas Turbine & Aeroengine Congress & Exhibition
Orlando, Florida — June 2–June 5, 1997

Leakage flow occurs primarily in the clearance region between rotor-tip and casing (and also between the stator blade and hub). Detailed measurements on turbine blade profiles have been reported by many authors including: Moore and Tilton(1988); Bindon(1989); Yaras and Sjolander(1989); Storer and Cumpsty(1991); Heyes and Hodson(1993); Kang and Hirsch(1994); Cecco et al.(1995). These investigators, and others, have—for incompressible flow—provided a detailed description of the flow structure around the tip region, sometimes taking account of tip profiling and moving adjacent walls. Recent experimental work by Wehner et al.(1996) has extended this data base into the transonic regime.

Prediction and modelling of tip leakage flow falls into four main categories: momentum based models; energy based models; models which apply a mixing analysis; and Reynolds Averaged Navier-Stokes(RANS) calculations. An overview of literature covering the first three categories has been presented by Yaras and Sjolander(1992). We, will focus on more recent developments in the fourth category.

Storer and Cumpsty(1991) used the structured code developed by Dawes (see also Dawes, 1987) with 50k cells[1], to help with interpretation of their experimental work. Despite a very crude representation of the tip gap region (applying periodicity along six cells spanning the gap), they obtained surprisingly good agreement between measurements and calculations—thus inferring that tip leakage losses are dominated by inviscid flow phenomena, which can to a first approximation be captured by consideration of massflow and momentum through a suitable control volume, as originally proposed by Denton and Cumpsty(1987). The same code was applied by Perrin et al.(1992) on a supersonic axial flow compressor using 150k cells— with 10 cells spanning the gap.

Liu and Bozzola(1993) used their own H-mesh solver on a low Mach number linear turbine cascade, with about 90k cells, of which 2500 where inside of the tip region.

Suder and Celestina(1994) presented comparisons between laser anemometer measurements and calculations (for description of their code see Adamcyzk et al.,1989) on the NASA Rotor-37. Such data from rotating machines at equivalent Mach and Reynolds numbers is very useful. However the CFD challenge is emphasized by the fact that despite using over 260k cells, they could only afford to place two cells radially between the tip and the casing.

An investigation for incompressible flow was published by Basson and Lakshminarayana(1995) employing an embedded H-mesh. Using this approach with 260k cells, they were able to place 12k cells within the tip gap region, thus resolving some of the detail.

In the present study we include results with a parallel unstructured RANS code using nearly 2 million cells: refinement has allowed us to put around 200k cells specifically in the tip gap region.

[1]Here structured means the mesh is generated in a sequential manner—in this case it was an H-mesh having about 50,000 cells.

BRIEF OVERVIEW OF THE PARALLEL CODE

The code has been developed from the unstructured algorithm originally presented by Dawes(1993). We solve the conservation integral form of the Reynolds-Averaged Navier-Stokes equations comprising of continuity, momentum in three directions, and energy. In addition turbulence is modelled by low-Reynolds number $k-\epsilon$ equations (Patel et al., 1985). The damping functions are based upon Lam and Bremhorst(1981), but modified to avoid explicitly evaluating wall proximity.

The present version has been discretized in a fully conservative manner using non-overlapping control volumes. The residual terms are calculated by considering flux through faces associated with edges between nodes, as opposed to the earlier formulation which calculated flux through faces of each tetrahedral cell. The artificial dissipation term proposed by Jameson(1985) is used, together with the modified scaling factors presented by Martinelli(1987).

Integration to a steady-state solution is performed using an explicit 4-stage Runge-Kutta scheme, with viscous and artificial dissipation terms calculated only on the first stage.

The parallel code comprises a parent program running on a large workstation or our Cray Y-MP, together with the children which are spawned onto a specified number of pre-enrolled workstations, or typically 64 processors (PE's) on the Cray T3D. The parent is responsible for reading the data files, partitioning the mesh, and spawning the child processes. The children solve the flow on their local mesh. Inter-processor communication is handled via PVM or Cray specific message passing libraries. For further detail see Hustad and Vilmin(1997).

TEST CASE NUMBER 1

Experimental measurements have been conducted by Wehner(1996) investigating tip clearance effects using flat plates in a linear transonic tunnel. The initial computational mesh is shown in Fig.1.

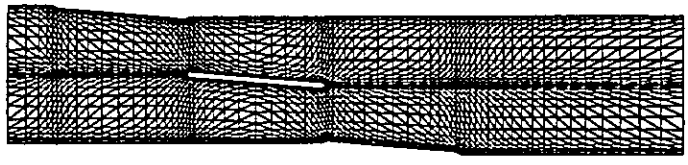

Figure 1: Midspan View of Starting Mesh with 190k Cells.

The actual experimental configuration shown in Fig.2 comprises 3 staggered blades with: cbord(c) 100mm; span 100mm; thickness 4mm; mounted horizontally at 5° incidence in the transonic working section. The tip-gap height(τ) for the centre blade(no.2) could be adjusted by moving the blade spanwise. The present study considers results for a gap height of 6mm.

The test section was complicated by the abrupt termination of the ceiling. For this reason, and in order to slightly simplify the flow domain, the computational mesh extends only between blade no.1 and no.3.

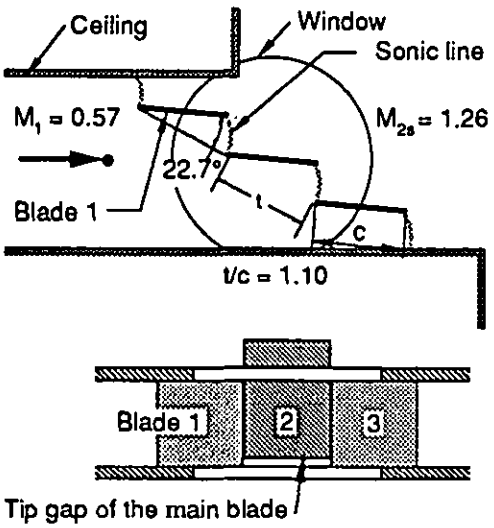

Figure 2: Experimental Configuration for Case Number 1.

To obtain the correct pressure distribution over blade no.2, we modified the upper and lower boundaries as shown by the refined mesh in Fig.3. Here, the bottom surface has been lowered 4mm and profiled to mimick the path of the stagnation streamline impinging onto blade no.3. In a similar manner the upper surface represents the stagnation streamline in the wake from behind blade no.1.

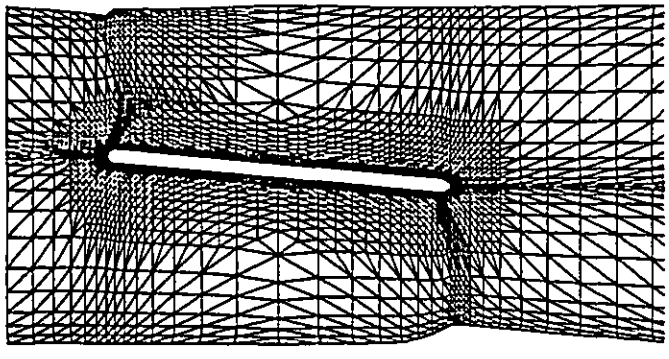

Figure 3: Refined Mesh at 90% Span with 720k Cells.

Our criterion for doing tbis modification is simply comparison with the available experimental pressure distribution over blade no.2 at 90% span, as shown in Fig.4. Tip leakage flow is primarily driven by pressure difference between the suction and the pressure surface—the good agreement is however not a validation of the code, but simply a pre-requisite prior to investigating flow within the tip gap region itself.

After refining we estimate there is about 30k cells within the gap. This intermediary level of refinement is not sufficient to ensure a wholly grid independent solution, but does allow for realistic comparisons with the laser-2-focus velocity data measured within the gap.

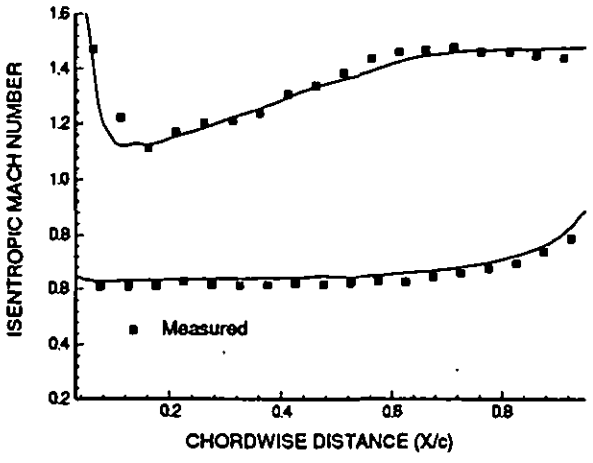

Figure 4: Calibration of Computational Mesh Using Calculated and Measured Pressure Distribution at 90% Span.

Figure 5 shows the chordwise variation of tip gap velocity and flow angle, along the gap centreline, ie. 3mm from both the wall and the tip, in the mid-blade plane. The solid line is calculated velocity (plotted in m/s for direct comparison with the hollow squares which are measured values). The dashed line is flow angle which can be compared with the solid triangles. For a large part of the chord, not only trends, but also magnitudes compare rather well. After 80% chord there is a noticeable discrepancy in comparison of velocities which we discuss later.

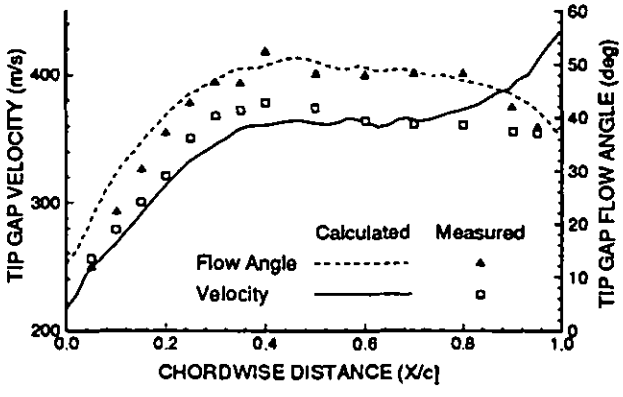

Figure 5: Comparison of Calculated and Measured Velocity and Flow Angle Along the Gap Centreline.

An important feature of the flow is the extent to which free-stream total pressure establishes itself witbin the tip gap region—most tip leakage models presume this to be the case. Figure 6 presents the variation of total pressure along the gap centreline (non-dimensionalized using the free stream value), for two different inflow boundary-layer profiles: Run-1 (solid line) is the case at hand; Run-2 will be mentioned later. The initial value of total pressure near the leading edge, is determined by the state of the incoming

wall boundary-layer profile. However by about 30% chord, the total pressure is within two percent of the free stream value. This coincides with the levelling-off of the flow angle at about 48°, as already seen in Fig.5.

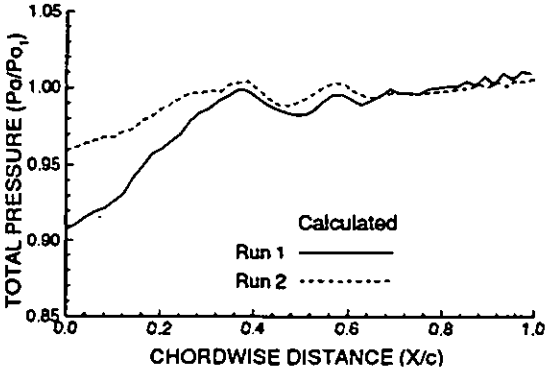

Figure 6: Calculated Chordwise Variation of Total Pressure Along the Gap Centreline.

A more detailed view of flow development is revealed by contour plots in the pitchwise plane. Figure 7 shows the outer half span at 20% chordwise location: graduations along the lower edge of the figure are every 2mm. The boundary layer over the blade and sidewall is made evident by the reduced contour values in these regions. The tip gap flow is moving from the lower (pressure) onto the upper (suction) surface. In the gap, the total pressure originally within the sidewall boundary-layer, is beginning to be pushed out by the flow from below. Separation—from the pressure surface corner—and a tip vortex (suction surface corner), are just starting to develop.

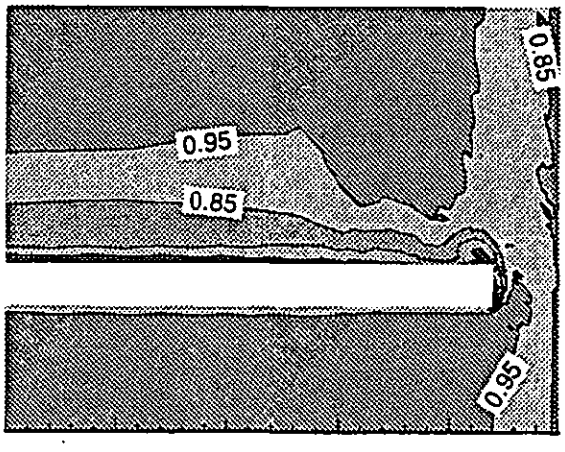

Figure 7: Calculated Non-Dimensional Stagnation Pressure Contours in Pitchwise Plane at 20% Chord.

A similar image at 80% chordwise location is shown in Fig.8. There is now a well established separated flow region immediately adjacent to the tip surface, together with a strong shear layer rolling up to form the leakage vortex. The slightly jagged nature of the contour lines is an indica-

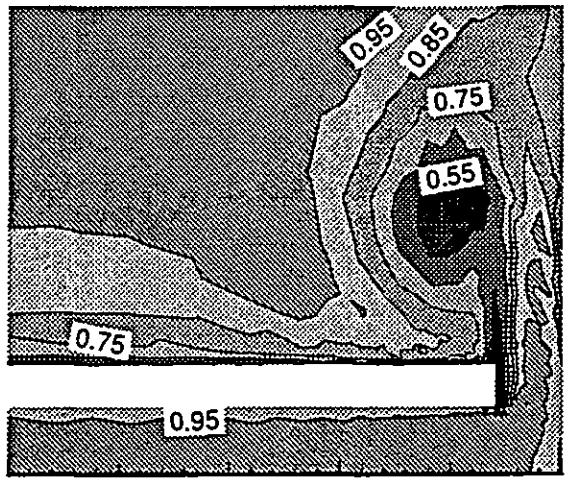

Figure 8: Calculated Non-Dimensional Stagnation Pressure Contours in Pitchwise Plane at 80% Chord.

tion that the numerical dissipation has been reduced to a minimum permissible level. A substantial part of the gap is now occupied by the free-stream flow which enters with a velocity of 300m/s (Mach 0.95) and leaves the gap at 430m/s (Mach 1.4). This—together with the shear layer adjacent to the tip surface—emphasises the high velocity gradients existing in the region, and could readily explain the discrepancies in comparison between velocities, observed towards the trailing edge in Fig.5.

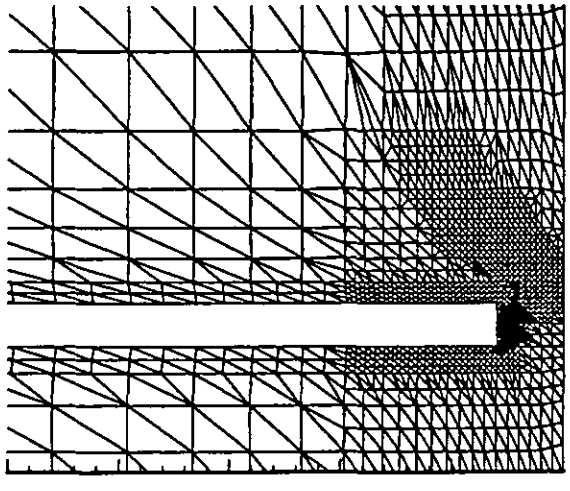

Figure 9: Mesh in Pitchwise Plane at 80% Chord.

The mesh varies streamwise, but a representative cross-section is shown in Fig.9 at 80% chordwise location. Refinement was based upon entropy gradient to improve resolution around the vortex and shear-layer. The shear layer adjacent to the tip surface is well resolved, however the mesh is still too coarse to provide any useful (grid independent) comparisons for loss prediction. The sidewall boundary layer is also coarse in places: a second (clockwise rotat-

ing) vortex, which should exist between the boundary layer and the emerging tip gap flow, is not apparent (see Wehner et al., 1996). The slight lifting away from the sidewall of the contour near the top right of Fig.8 may be interpereted as the start of this process.

TEST CASE NUMBER 2

Investigation into tip flow on the outer profile from the last-stage blade of a low-pressure steam turbine, were conducted by Wehner(1996) using the annular cascade test facility at EPFL (Bölcs, 1983). The hub radius was 160mm and the outer casing was 200mm. There were 16 blades (with chord 75mm) uniformly distributed about the circumference.

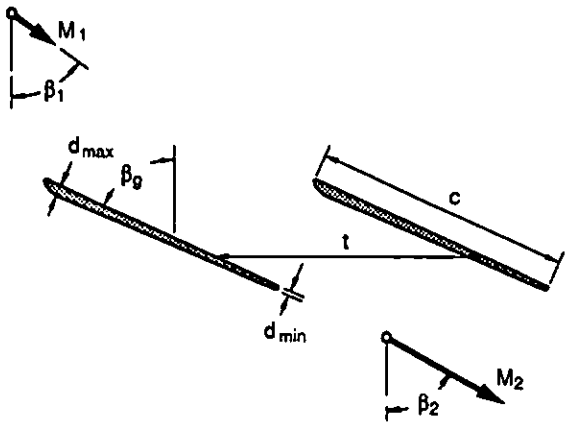

Figure 10: Blade Configuration in the Annular Cascade.

A sketch of the test arrangement is shown in Fig.10. Apart from the profiled leading edge region, both surfaces are nearly straight with maximum thickness of 3.0mm at 7% chord: this decreases steadily ending in a trailing edge diameter of 1.7mm. The geometric angle β_g was 65.9°. Comparisons have been done for one test (no.811) using: tip-gap height(τ) 1.0mm; nominal inflow angle $\beta_1 = 52.0°$; isentropic exit Mach number 1.40; total pressure 209kN/m^2. The measured profiles for total temperature, total pressure and flow angle were imposed at the inlet plane. A linear variation (from hub to casing) of static pressure, based on measured values, was fixed at the outlet plane.

The comparatively coarse midspan mesh (in comparison to sections closer to the tip), is shown in Fig.11. In total the mesh contains 1.8 million cells—with the majority of these being refined using pressure and entropy gradients, to resolve the tip gap and endwall flow. We estimate that there are at least 200k cells within the gap region between the blade tip and casing

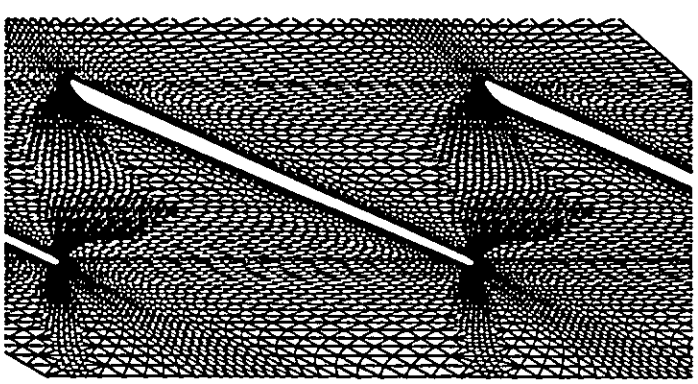

Figure 11: Midspan Mesh Containing 1.8 million Cells.

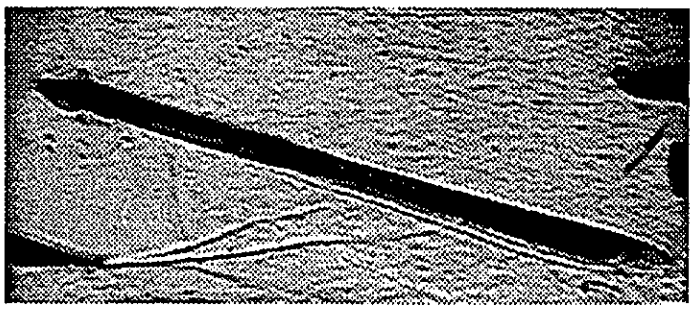

Figure 12: Schlieren Image of Flow Field.

A Schlieren image of the flow field is reproduced in Fig.12. The profile is somewhat distorted due to the curvature of the annular cascade. Nevertheless the image gives a reasonable impression of the flow moving from top left to bottom right. An oblique trailing edge shock is shown by the two nearly horizontal lines from the TE in the bottom left corner. These coincide with the shock/boundary-layer interaction along the hub and casing walls. A fainter vertical line traverses the passage suggesting a slightly oblique compression wave which interacts with the suction surface at about 20% chordwise location. Closer inspection also reveals a line associated with the tip leakage flow, appearing at about 10% chord, curving downwards and out into the blade passage. The image can be compared with the midspan Mach number contours shown in Fig.13.

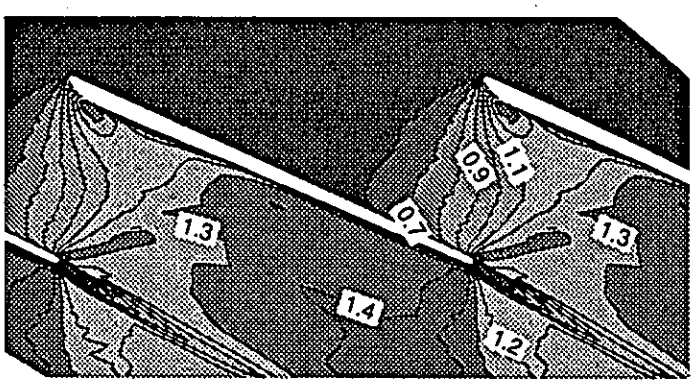

Figure 13: Midspan Mach Contours.

However for detailed comparison it is better to consider the chordwise static pressure distribution shown in Fig.14 at two spanwise locations—again we have used absolute units of mbar for a direct comparison.

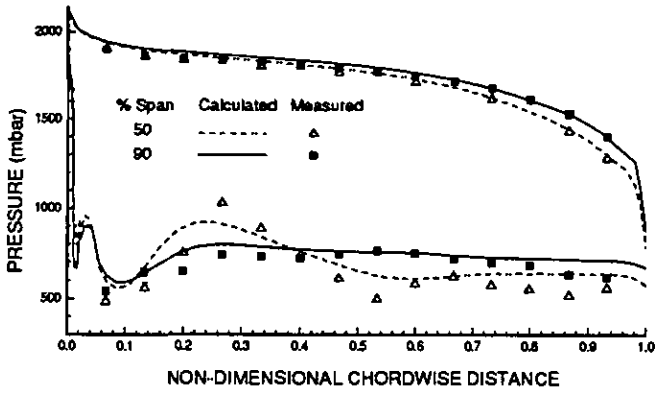

Figure 14: Comparison of Calculated and Measured Pressure Distribution at 50% and 90% Spanwise Location.

The upper lines along the pressure surface compare very well at both spanwise positions. At midspan on the suction surface the lower dashed line can be compared with the bollow triangles. The Mach contours in Fig.13 show that tbe main flow remains supersonic, hence the rise and fall of the pressure from 10 to 50% chord, reflect a weak compression and expansion which the flow experiences on leaving the passage between the blades. At 60% the oblique TE shock is just visible in the measurements. The calculated pressure is slightly smeared, but nevertheless the trends are similar. In particular the more uniform distribution at 90% span is well predicted.

DISCUSSION OF RESULTS

To help identify important features of the tip leakage flow, we have—for both cases—modified the incoming sidewall boundary layer. For each condition the resulting non-dimensional total pressure profile has been plotted versus distance from sidewall (in units of tip gap height), as shown in Fig.15. For Case No.1/Run-2 the boundary layer at inlet was removed, resulting in a much thinner region of lower

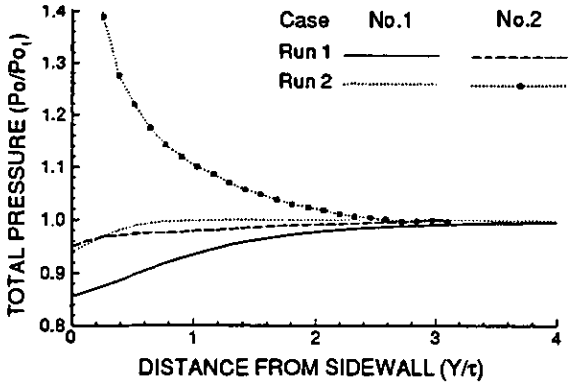

Figure 15: Comparison of Non-Dimensionalized Sidewall Boundary-Layer Profiles for all Four Cases Presented.

total pressure approaching the gap (dotted line). The effect this had on chordwise development within the gap has already been shown by the dashed line in Fig.6—the leakage flow is able to establish itself more rapidly.

With Case No.2 in the annular cascade, gap aspect ratio is lower and we observe that the separated flow adjacent to the blade-tip surface occupies a proportionately larger part of the gap height. The free stream flow is not able to fully penetrate into the gap, as shown by the solid line in Fig.16.

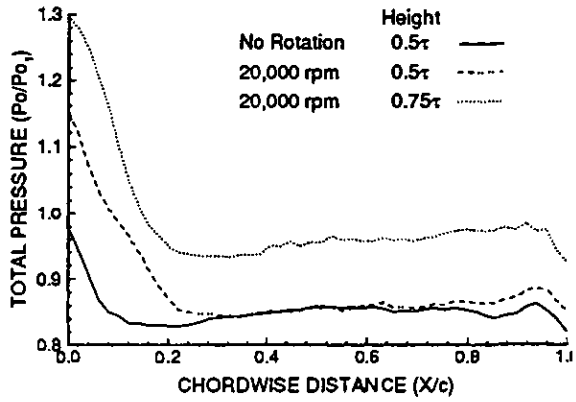

Figure 16: Chordwise Variation of Total Pressure in the Gap for Case No.2—With and Without Rotation.

The final comparison, Case No.2/Run-2, is with a rotating adjacent sidewall. The direction of rotation (from suction to pressure side) is as would be experienced by a turbine. The speed of rotation (20,000 rpm) is based upon exit velocity and flow angle to ensure that the flow leaves the last-stage at approximately zero degrees[2].

In our fixed frame of reference, the effect of rotation on the flow entering the tip gap region is to increase the total pressure above the free stream value, as shown in Fig.15. Development of total pressure along the gap centreline is presented in Fig.16 by the dashed line. Most noticeable is that in both cases (with and without rotation), by 20% chordwise location, the pressure has established itself at the same level independent of whether the adjacent wall is moving or not. However the third (dotted) line shows that total pressure variation closer to the wall is now much higher.

The overall effect of this on development of the tip leakage vortex can be seen in Fig.17 showing a pitchwise view of entropy contours[3] at 50% chordwise location. The view on the left (no rotation) reveals that the leakage vortex moves further out along the endwall into the passage, compared with the view on the right where the relative motion of the wall retains the leakage flow.

A final point to note for both test configurations investigated during the present study, is that the rapid acceleration of the tip jet through the gap leads to locally supersonic

[2]Usually there is a large diffuser behind this stage, and one would design for a minimum of swirl.

[3]Here, these are virtually equivalent with the non-dimensional total pressure contours used previously.

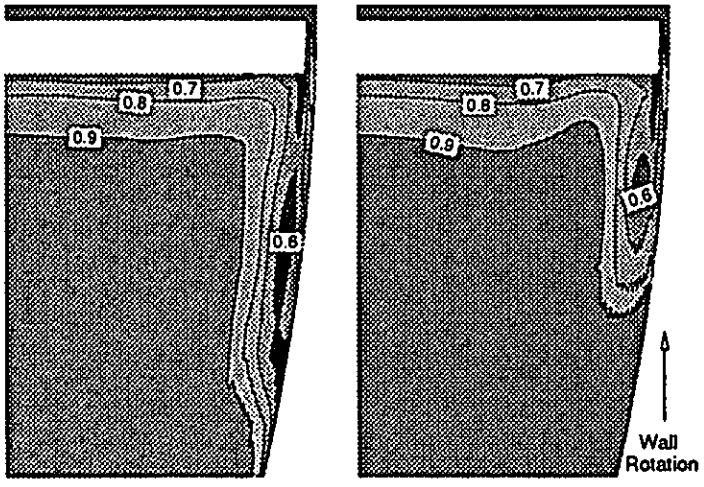

Figure 17: Comparison of Tip Leakage Flow for Case No.2—With and Without Rotation of Adjacent Sidewall.

flow conditions. An example of this is shown in Fig.18 by the Mach contours at mid-gap height for Case No.1. The projected profile of the blade has been superposed on the image. The Mach 1 line emerges from the gap near 30% chord location at about 15° with respect to the main flow.

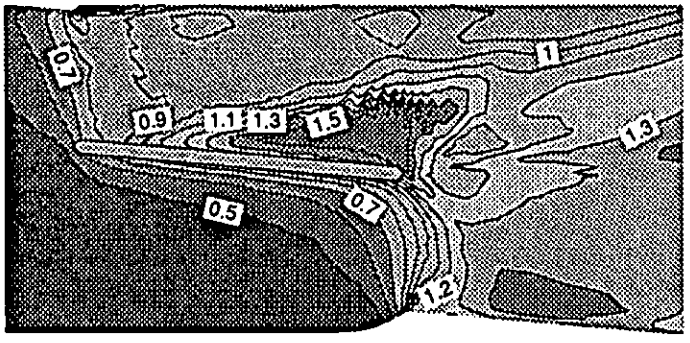

Figure 18: Mach Contours at 0.5τ from Sidewall for Case No.1/Run-1.

For Case No.2 a similar observation may be had from the Schlieren image in Fig.12, where we have already mentioned the faint—but distinctive—line evident from about 10% chordwise location. Comparison with calculated contours at mid-gap height in Fig.19 reveal that the Mach 1 line shows a similar trend.

Exactly where the shock resides depends on the tip geometry and main flow conditions. In certain situations (eg. flow re-attachment within the gap) the return to subsonic conditions may occur in the gap itself, due to expansion following the initial *vena contracta*, as suggested by Wehner et al.(1996) for Case No.1 using a tip gap of 3mm.

However, if the main flow is also supersonic, then there may be no need for a local tip-leakage shock. Although this will also depend on whether the tip is actually buried within the subsonic region of the endwall boundary layer.

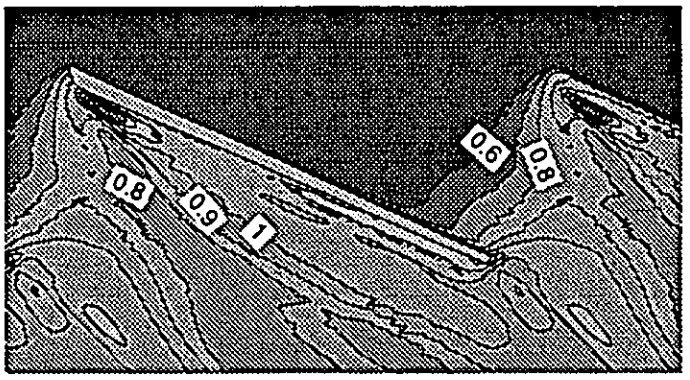

Figure 19: Mach Contours at 0.5τ from Sidewall for Case No.2/Run-1—No Rotation.

Using the model proposed by Wehner et al.(1997) on Case No.1 with gap height 3mm, the predicted leakage loss (ζ_{gap}) increased from 0.041 to 0.052, when including the additional entropy generation due to a shock within the gap. Wehner et al.(1997) originally underpredicted losses for test Case No.2 in the annular cascade, and therefore included an empirical factor increasing the tangent of the flow angle by 1.13. To achieve a similar correction using the modified loss value obtained for Case No.1, resulted in a factor of 1.18. Thus suggesting that the empiricism may have been necessary because the model did not include provisions for local tip-leakage shock loss.

CONCLUSIONS

One of the goals of this paper has been to show how moving onto parallel computers can improve the potential quality of our results. We demonstrate the practical application of a parallel unstructured Navier-Stokes code to help with interpretation of transonic tip leakage flows. Comparisons with the available experimental data is good. We do not include estimates for overall loss predictions because we still observe a grid dependent solution which is also sensitive to the level and implementation of the numerical dissipation. Furthermore we believe that grid quality, cell aspect ratio, improved profile definition, and better adaption criteria are all aspects of the work which need to he considered before any really meaningful loss values can be presented. Despite this we show how free stream total pressure establishes itself within the gap region; investigate the influence of a moving adjacent wall; and discuss the occurrence of localized tip-leakage shock formation and its possible influence on overall loss prediction.

ACKNOWLEDGEMENT

The experimental work has received financial support from the "Nationaler Energie-Forschungs-Fonds" (NEFF) and ABB Power Generation Ltd., Baden, Switzerland.

Development of parallel computing at LTT is currently funded by the Fonds National Suisse (project No. 21-37330-93).

REFERENCES

Adamcyzk J.J., Celestina M.L., Beach T.A., Barnett M., 1989, "Simulation of Three-Dimensional Viscous Flow Within a Multi-Stage Turbine", ASME Journal of Turbomachinery, Vol.112, pp.370-376.

Ainley D. G., Mathieson G. C. R., 1951, "A Method of Performance Estimation for Axial-Flow Turbines", Aeronautical Research Council R&M No.2974.

Basson A., Lakshminarayana B., 1995, "Numerical Simulation of Tip Clearance Effect in Turbomachinery", ASME Journal of Turbomachinery, Vol.117, pp.348-359.

Bindon J. P., 1989, "The Measurement and Formation of Tip Clearance Loss", ASME Journal of Turbomachinery, Vol.111, pp.257-263.

Bölcs A., 1983, "A Test Facility for the Investigation of Steady and Unsteady Transonic Flows in Annular Cascades", ASME-Paper 83-GT-34.

Cecco S.D., Yaras M.I., Sjolander S.A., 1995, "Measurements Of The Tip-Leakage Flow In A Turbine Cascade With Large Clearances", ASME-Paper 95-GT-77

Dawes W.N., 1987, "A Numerical Analysis of the Three-Dimensional Viscous Flow in a Transonic Compressor Rotor and Comparison with Experiment", ASME Journal of Turbomachinery, Vol.109, pp.83-90.

Dawes W.N., 1993, "The Extension of a Solution-Adaptive Three-Dimensional Navier-Stokes Solver Towards Geometries of Arbitrary Complexity", ASME Journal of Turbomachinery, Vol.115, pp.283-295.

Denton J. D., Cumpsty N. A., 1987, "Loss Mechanisms In Turbomachines", Proc. Inst. Mech. Engrs., Cambridge, 1-3 Sept. pp.1-14.

Denton J.D., 1993, "Loss Mechanisms In Turbomachines", ASME Journal of Turbomachinery, Vol.115, pp.621-656.

Heyes F. J. G., Hodson H.P., 1993, "Measurement and Prediction of Tip Clearance Flow in Linear Turbine Cascades", ASME Journal of Turbomachinery, Vol.115, pp.376-382.

Howell A. R., 1945, "The Design of Axial-Flow Compressors", Proc. IMechE., Vol.153.

Hustad C-W., Vilmin S., 1997, "A Parallel Unstructured Turbomachinery Code", To be presented, ASME Conference, Orlando, Florida.

Jameson A., 1985, "Numerical Solution of the Euler Equations for Compressible Inviscid Fluids", In *Numerical Methods for the Euler Equations of Fluid Dynamics*, Angrand F., Dervieux A., Desideri J.A., Glowinski R., ed., SIAM.

Kang S., Hirsch C., 1994, "Tip Leakage Flow in Linear Compressor Cascade", ASME Journal of Turbomachinery, Vol.116, pp.657-664.

Lam C.K.G., Bremhorst K.J., 1981, "Modified Form of k-epsilon Model for Predicting Wall Turbulence", Journal of Fluid Engineering, Vol.103, pp.456-

Liu J.S., Bozzola R., 1993, "Three-Dimensional Navier-Stokes Analysis of Tip Clearance Flow in a Linear Turbine Cascade", AIAA Journal, Vol.31, No.11, pp.2068-2074.

Martinelli L., 1987, "Calculations of Viscous Flows with a Multigrid Method", Ph.D. Thesis, Department of Mechanical and Aerospace Engineering, Princeton University.

Moore J., Tilton J.S., 1988, "Tip Leakage Flow in a Linear Turbine Cascade", ASME Journal of Turbomachinery, Vol.110, pp.18-26.

Patel V.C., Rodi W., Scheurer G., 1985, "Turbulence Models for Near-Wall Flows and Low Reynolds Numbers: a Review", AIAA Journal, Vol.23, pp.1308-1319.

Rains D. A., 1954, "Tip Clearance Flows in Axial Flow Compressors and Pumps", California Institute of Technology, Hydrodynamics and Mechanical Engineering Laboratories, Report No.5.

Perrin G., Leboeuf F., Dawes W.N., 1992, "Analysis of Three-Dimensional Viscous Flow in a Supersonic Axial Flow Compressor Rotor with Emphasis on Tip Leakage Flow", ASME Paper 92-GT-388.

Suder K.L., Celestina M.L., 1994, "Experimental and Computational Investigation of the Tip Clearance Flow in a Transonic Axial Compressor Rotor", ASME-Paper 94-GT-365.

Storer J.A., Cumpsty N.A., 1991, "Tip Leakage Flow in Axial Compressors", ASME Journal of Turbomachinery, Vol.113, pp.252-259.

Yaras M.I, Sjolander S.A., 1989, "Losses in the Tip-Leakage Flow of a Planar Cascade of Turbine Blades", Paper 20, AGARD-CP-469.

Yaras M.I., Sjolander S.A., 1992, "Prediction of Tip-Leakage Losses in Axial Turbines", ASME Journal of Turbomachinery, Vol.114, pp.204-210.

Wehner M., 1996, "Experimentelle und theoretische Untersuchung der Spaltströmung in einer Turbine bei Überschallabströmung", Ph.D. Thesis. EPFL, Switzerland.

Wehner M., Bölcs A., Bütikofer J., 1996, "Experimental Study of Tip Clearance under Transonic Flow Conditions", ASME-Paper 96-GT-99.

Wehner M., Bütikofer J., Hustad C-W., Bölcs A., 1997, "Measurement and Prediction of Tip Leakage Losses in an Axial-Flow Transonic Turbine", To be presented, ASME Conference, Orlando, Florida.